

Spatial Dark-Soliton Stripes and Grids in Self-Defocusing Materials

G. A. Swartzlander, Jr.,^{(1),(a)} D. R. Andersen,⁽²⁾ J. J. Regan,⁽²⁾ H. Yin,^{(1),(b)} and A. E. Kaplan⁽¹⁾

⁽¹⁾*Department of Electrical and Computer Engineering, The Johns Hopkins University, Baltimore, Maryland 21218*

⁽²⁾*Department of Electrical and Computer Engineering, The University of Iowa, Iowa City, Iowa 52242*

(Received 22 December 1989)

Spatial dark-soliton (SDS) stripes are experimentally found in the transverse plane of a laser beam that passes through a rectilinear diffraction screen before propagating in a self-defocusing nonlinear material. Materials with different mechanisms of nonlinearity manifest the same qualitative results. The SDS nature of the observed phenomenon is verified by numerical simulations of the (2+1)-D nonlinear Schrödinger equation, analytical solutions for the (1+1)-D case, and their comparison with experimental data.

PACS numbers: 42.30.-d, 42.10.Qj, 42.50.Qg, 42.65.Jx

Dark solitons¹ have provoked much interest²⁻⁹ since they were first shown to be particular solutions of the two-dimensional (1+1)-D nonlinear Schrödinger equation (NSE) with a negative (self-defocusing-type) nonlinear coefficient n_2 [see Eq. (1) below]. As opposed to a so-called “bright” NSE soliton, which propagates as a stationary wave packet of finite extent in a (1+1)-D nonlinear medium with $n_2 > 0$, a “dark” soliton is characterized as a stationary “hole” on an otherwise uniform plane wave—it exists on a background field as an absence of energy in a localized region, with constant size and shape parameters, and remarkable stability. So far, only (1+1)-D *temporal* dark solitons (i.e., intensity minimums propagating along a nonlinear fiber on a quasi-cw bright background) have been observed experimentally.⁴⁻⁷ Here we report the first observations (see also Ref. 10) of stable *spatial* structures (e.g., stripes, crosses, and grids) in the transverse cross section of a cw optical beam propagating in a material with a self-defocusing nonlinearity, with these structures having a strongly pronounced soliton nature—namely, that of spatial dark solitons (SDS’s). Although no (2+1)-D analytical solution for dark solitons in the NSE is known to date, our experimental and numerical data with various 2D amplitude and phase masks provide strong evidence that the phenomenon observed by us is indeed due to spatial dark solitons. Furthermore, our results here on quasi-(1+1)-D propagation (see also Ref. 11) have shown excellent agreement with the well-known analytical results for (1+1)-D dark solitons.¹

SDS’s constitute a fundamental phenomenon, which, in the (1+1)-D case, is mathematically isomorphic to temporal dark solitons in the same way as, for example, (1+1)-D self-trapped channels in a self-focusing material are isomorphic to temporal bright solitons in fibers—in both cases the related phenomena are described by the normalized NSE. In comparison to temporal solitons, however, SDS’s are easy to create and observe experimentally, requiring as little as a HeNe laser and some slightly absorbing fluid. Various applications of SDS’s can be envisioned, such as optical encoding, limiting, switching and computing, and nonlinear filtering.

Our exploration into SDS formation was motivated by the observation of intriguing nonlinear transformations of far-field (Fraunhofer) diffraction patterns of a wire mesh placed at the input face of a sodium-vapor cell [see Fig. 1 and Fig. 2(a), column 1]. (Far-field diffraction is highly sensitive to intensity-dependent phase changes in a nonlinear layer.¹²) In all the cases studied so far with rectilinear diffraction screens, the linear Fraunhofer diffraction pattern evolves into various arrays of square spots as the laser intensity increases. Subsequent measurements at the output face of the nonlinear medium (in the Fresnel or near-field regime) revealed the formation of very distinct dark stripes which had caused those novel nonlinear far-field patterns.

In our initial experiment¹⁰ a cw frequency-stabilized dye laser beam of power $P_{in} \sim 100$ mW (Fig. 1) was passed through a wire mesh and then imaged with a 100-mm focal-length lens into an $L = 18$ -mm-long cell containing $\sim 10^{12}$ atoms/cm³ of sodium vapor, which is known to be a strongly nonlinear material (see, e.g., Ref. 13). The laser frequency was tuned slightly below the D_2 atomic resonance, corresponding to a negative nonlinearity ($n_2 < 0$). By using the self-deflection effect,¹⁴ the strongest resonantly enhanced negative nonlinear coefficient n_2 was measured to be $\approx -3 \times 10^{-7}$ cm²/W.¹⁵ The square mesh apertures had a size of $x_B = 160$ μ m and wires of diameter $x_A = 160$ μ m. The Gaussian beam, with a radial (e^{-2}) beam size of $w_0 \sim 220$ μ m, was dissected into a $\sim 3 \times 3$ array of spots (see Fig. 2,

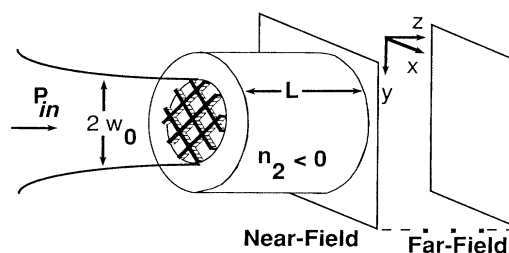


FIG. 1. A laser beam is incident on a wire mesh at the input face of a self-defocusing medium. Cross-sectional images are recorded in the near-field and far-field planes.

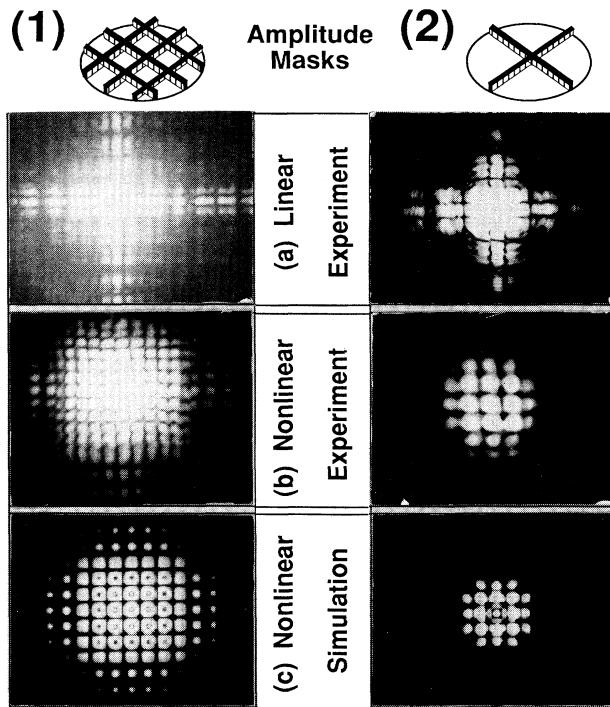


FIG. 2. Far-field cross-sectional images for propagation through sodium vapor with a wire mesh in the incident plane (column 1) and through an absorbing liquid with the "cross" configuration (column 2).

column 1). Far-field intensity profiles were recorded at a distance of > 1 m. The spectacular transformations of the far-field patterns described above were observed when the laser was scanned from an off-resonance frequency, below the D_2 transition frequency, toward the resonance (thereby varying the value of n_2). Fraunhofer diffraction was observed [see Fig. 2(a), column 1] far off resonance, where $n_2 \approx 0$. However, as the laser frequency approached the D_2 line (from below), the far-field profile transformed itself into an amazingly well-organized square array of spots, filling the central area of the beam, Fig. 2(b), column 1. (At the self-focusing side of the D_2 line, where $n_2 > 0$, the transformation was considerably different from that described above and consistent with the earlier results for self-focusing materials.¹⁶)

The geometric beauty of the far-field patterns and their stability over a relatively large range of intensities and driving-field frequencies led us to believe that this phenomenon is not attributed to the specific physics of the nonlinearity in sodium vapor, but rather to the simple fact that the nonlinear component of the refractive index is negative, i.e., $n_2 < 0$. To verify this, we tried an experiment using another phenomenon resulting in large values of $n_2 < 0$: the so-called thermal nonlinearity, which can readily be induced using low-power radiation

in many slightly absorptive liquids. The results of these experiments showed nonlinear far-field patterns amazingly similar to each other and to those of the sodium-vapor experiment. Although the nonlinearity due to the thermal effect exhibits some spatial nonlocality, this has not appreciably affected the observed phenomenon, presumably because the characteristic scale of the nonlocality was smaller than the soliton size.

The simplest and probably most fundamental wire mesh configuration is a single opaque "cross" (see Fig. 2, column 2). In this case the Fraunhofer pattern [Fig. 2(a), column 2] experiences a nonlinear transformation into a grid pattern [Fig. 2(b), column 2] that has essentially the same characteristics as the 3×3 mesh case (except that there are fewer spots), indicating similar nonlinear transformations in both cases.

To understand the observed phenomenon, we modeled the experiment using the (2+1)-D NSE for laser beam propagation in a nonlinear medium:

$$2ik \partial E / \partial z + \nabla_{\perp}^2 E + k^2 n_2 |E|^2 E / n_0 = 0, \quad (1)$$

where $\nabla_{\perp}^2 = \partial^2 / \partial x^2 + \partial^2 / \partial y^2$ [$= \partial^2 / \partial x^2$ for the (1+1)-D NSE], x and y are the transverse coordinates, z is the propagation coordinate, E is the complex electric field, and k is the wave vector in the material. Equation (1) was solved by us using numerical methods.¹⁷ The simulated far-field results [see Fig. 2(c)] show the same features as the experimental far-field patterns in Fig. 2(b). The agreement between the experimental and numerical results is remarkable.

To identify the physical phenomenon which gave rise to the observed *far-field* patterns, we studied the specific features of wave propagation *inside* the nonlinear material. This was accomplished by examining the *near-field* patterns at the output face of the nonlinear material for different lengths of the material, and for various boundary conditions, including a single wire, two parallel wires, two orthogonal sets of parallel wires, a wire mesh, a single phase jump, multiple phase jumps intersecting at a point, and two parallel phase jumps.¹⁰ The formation of pronounced dark stripes or grids was a universal phenomenon for all the cases studied. In general, the width of each stripe remained almost constant as the thickness of the nonlinear material increased, but decreased as the laser field strength increased. The number of these dark stripes, which tend to appear in pairs, also remained *constant* with propagation distance, even after collisions. These observations, together with the fact that $n_2 < 0$, suggest that the dark stripes are *spatial dark solitons*. Our investigation also shows that, notwithstanding orthogonal interactions, (2+1)-D dark-soliton stripes behave amazingly similar to the analytical (1+1)-D dark solitons;¹ i.e., it appears that soliton stripes orthogonal to each other in a cross-sectional plane propagate almost independently of each other.

To verify that the observed phenomenon was indeed

attributable to (2+1)-D dark solitons, we investigated the two most fundamental cases: (i) an opaque cross (“amplitude mask,” AM) composed of two orthogonal wires, and (ii) crossed phase steps (“phase mask,” PM) constructed with two microscope cover slips (see Fig. 3, columns 1 and 2). The corresponding near-field images are shown in Fig. 3 for a thermal nonlinear material. In the AM case, the linear Fresnel diffraction pattern [Fig. 3(a), column 1] exhibits a gray shadow of the cross flanked by bright stripes. In contrast, the shadow is completely missing in the experimental nonlinear profile [Fig. 3(b)]; instead, two high-contrast dark stripes, that are separated by a distinct bright region, are formed parallel to both axes of the cross. In spite of the magnification in size with increasing beam power due to self-defocusing, the width of the dark stripes actually decreases, as expected for dark solitons. In the PM case, the linear Fresnel diffraction pattern displays a broad dark cross aligned with the axes of the phase steps, flanked by diffractive ringing. As the laser power is increased [see Fig. 3(b), column 2], the width of the central cross decreases (even at the intersection) and does not split into two [as did the shadow of the dark opaque cross in Fig. 3(b)]. This also occurs in a (1+1)-D nonlinear system when the boundary condition is a π phase step,⁸ with the central dark stripe referred to as a “fun-

damental dark soliton”; similarly, the pattern in Fig. 3(b), column 2, can be regarded as a “fundamental dark-soliton cross.” Our numerical solutions for both nonlinear cases, shown in Fig. 3(c), again reaffirm that Eq. (1) correctly predicts the observed phenomena.

A strong verification of the soliton nature of the observed phenomenon was achieved by comparing¹¹ experimentally measured parameters with the theory. We measured the soliton divergence angle θ with respect to the optical axis (see inset of Fig. 4) to determine the soliton characteristic parameter $\lambda_{nl} = \theta \eta_{nl}^{-1/2}$ (the soliton amplitude and width also depend on λ_{nl}), where $\eta_{nl} \equiv |n_2||E|^2/2n_0$. When a single wire of diameter x_A is small compared to the beam size, then λ_{nl} is determined by the equation $\lambda_{nl} \approx \cos(\lambda_{nl}kA)$,¹ where $A = x_A \eta_{nl}^{1/2}$. The excellent agreement between the data and theory is shown in Fig. 4. The inset (Fig. 4) illustrates the formation of a pair of diverging dark solitons for the case of a single wire. To test the integrity of dark solitons on a *finite* (e.g., Gaussian) background, we computed the so-called “soliton constant”^{7,8} and found that this parameter was nearly constant ($= 1.76^2/n_0 n_2 k_0^2$). This indicated that these dark stripes propagate as robust formations, even though the background intensity relaxes adiabatically due to self-defocusing and linear diffraction [this is reminiscent of qualities of temporal dark solitons observed on a finite (1+1)-D Gaussian background in fibers⁷].

The *far-field* transformation of a linear Fraunhofer pattern into a tightly organized and ordered nonlinear pattern (as in Fig. 2) can now be explained in terms of

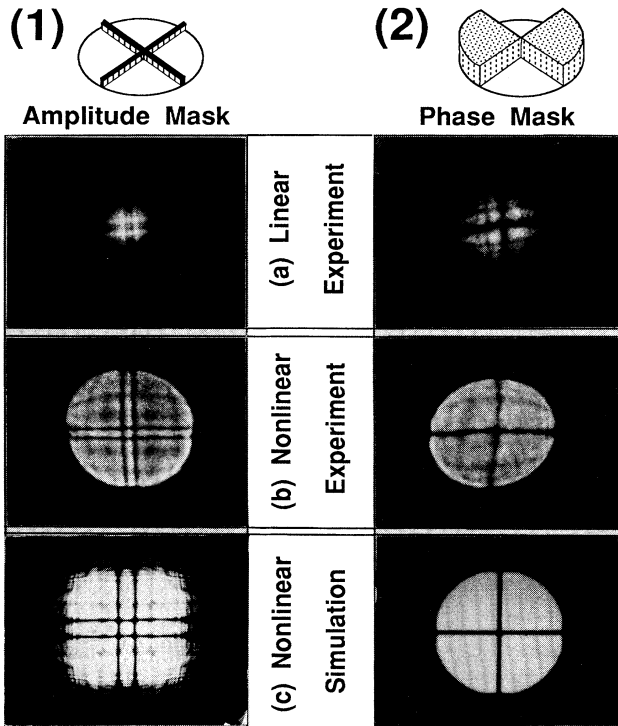


FIG. 3. Near-field cross-sectional images of the output sample face for propagation through an absorbing liquid with an amplitude cross (column 1) and a phase cross (column 2) in the incident plane.

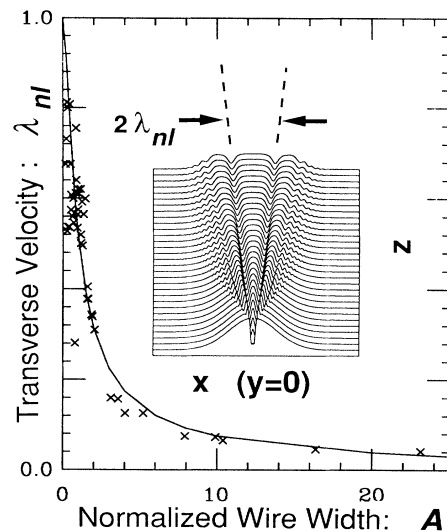


FIG. 4. Experimental (crosses) and theoretical values (solid line) of the soliton parameter λ_{nl} as a function of the normalized wire width A when the boundary condition is a wire that bisects a Gaussian beam. Inset: Corresponding numerical solution of the (2+1)-D NSE, showing intensity profiles in the plane, $y=0$, and a pair of diverging dark solitons.

the formation of spatial dark-soliton stripes and grids. This effect occurs, in general, because some spatial-frequency components of the incident beam are channeled into the formation of solitons, and thus are not allowed to "radiate" away from the optical axis as in the linear case.

In conclusion, we have observed the nonlinear transformation of various Fresnel and Fraunhofer diffraction patterns of a laser beam passing through a rectilinear amplitude or phase mask, followed by a self-defocusing material. Under nonlinear propagation, spatial dark solitons formed appearing as dark stripes or grids in the beam cross section. The (2+1)-D soliton structures behaved as if they consisted of two almost independent and noninteracting (1+1)-D soliton substructures. The similarity between our experimental data and numerical solutions of the (2+1)-D NSE was remarkable.

The work at Johns Hopkins University was supported by AFOSR, and that at Iowa by NSF. Computation was performed at the National Center for Supercomputing Applications and the Pittsburgh Supercomputing Center. We thank D. M. Pepper for suggestions on phase-cross measurements, Yu. S. Kivshar for discussions on soliton stability, and J. E. Bjorkholm for insights on sodium-vapor experiments. G.A.S. is an Office of Naval Technology Postdoctoral Fellow.

^(a)Presently at the Naval Research Laboratory, Code 6546, Washington, D.C. 20375-5000.

^(b)Presently at Tsinghua University, Beijing, People's Republic of China.

¹V. E. Zakharov and A. B. Shabat, *Zh. Eksp. Teor. Fiz.* **64**, 1627 (1973) [*Sov. Phys. JETP* **37**, 823 (1973)].

²A. Hasegawa and F. Tappert, *Appl. Phys. Lett.* **23**, 171

(1973).

³K. J. Blow and N. J. Doran, *Phys. Lett.* **107A**, 55 (1985).

⁴P. Emplit, J. P. Hamaide, F. Reynaud, C. Froehly, and A. Barthelemy, *Opt. Commun.* **62**, 374 (1987).

⁵D. Krökel, N. J. Halas, G. Giuliani, and D. Grischkowsky, *Phys. Rev. Lett.* **60**, 29 (1988).

⁶A. M. Weiner, J. P. Heritage, R. J. Hawkins, R. N. Thurston, E. M. Kirschner, D. E. Leaird, and W. J. Tomlinson, *Phys. Rev. Lett.* **61**, 2445 (1988).

⁷W. J. Tomlinson, R. J. Hawkins, A. M. Weiner, J. P. Heritage, and R. N. Thurston, *J. Opt. Soc. Am. B* **6**, 329 (1989).

⁸S. A. Gredeskul, Yu. S. Kivshar, and M. V. Yanovskaya, *Phys. Rev. A* **41**, 3994 (1990).

⁹L. J. Mulder and R. H. Enns, *IEEE J. Quantum Electron.* **25**, 2205 (1989).

¹⁰Some of these results were first reported in G. A. Swartzlander, Jr., and A. E. Kaplan, in *Proceedings of the 1989 Conference on Lasers and Electro-Optics (CLEO '89)*, Technical Digest Series Vol. 11 (Optical Society of America, Washington, DC, 1989); and in G. A. Swartzlander, Jr., D. R. Andersen, J. J. Regan, and A. E. Kaplan, in *Proceedings of the OSA Annual Meeting, Orlando, Florida, 1989*, postdeadline paper PD-7 (unpublished).

¹¹D. R. Andersen, D. E. Hooton, G. A. Swartzlander, Jr., and A. E. Kaplan, *Opt. Lett.* **15**, 783 (1990).

¹²A. E. Kaplan, *Izv. VUZ Radiofizika* **12**, 869 (1969) [*Radiophys. Quantum. Electron.* **12**, 692 (1969)].

¹³J. E. Bjorkholm and A. Ashkin, *Phys. Rev. Lett.* **32**, 129 (1974).

¹⁴A. E. Kaplan, *Pis'ma Zh. Eksp. Teor. Fiz.* **9**, 58 (1969) [*JETP Lett.* **9**, 33 (1969)].

¹⁵G. A. Swartzlander, Jr., H. Yin, and A. E. Kaplan, *Opt. Lett.* **13**, 1011 (1988); *J. Opt. Soc. Am. B* **6**, 1317 (1989).

¹⁶G. A. Askar'yan, Kh. A. Diyanov, and M. Mukhamad-zhanov, *Pis'ma Zh. Eksp. Teor. Fiz.* **16**, 211 (1972) [*JETP Lett.* **16**, 149 (1972)]; A. J. Campillo, S. L. Shapiro, and B. R. Suydam, *Appl. Phys. Lett.* **24**, 178 (1974).

¹⁷D. R. Andersen and J. J. Regan, *J. Opt. Soc. Am. A* **6**, 1484 (1989).

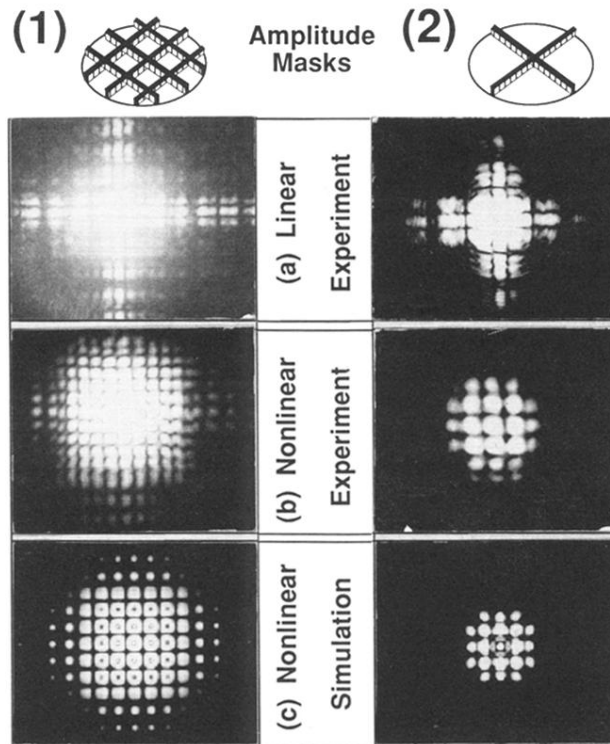


FIG. 2. Far-field cross-sectional images for propagation through sodium vapor with a wire mesh in the incident plane (column 1) and through an absorbing liquid with the “cross” configuration (column 2).

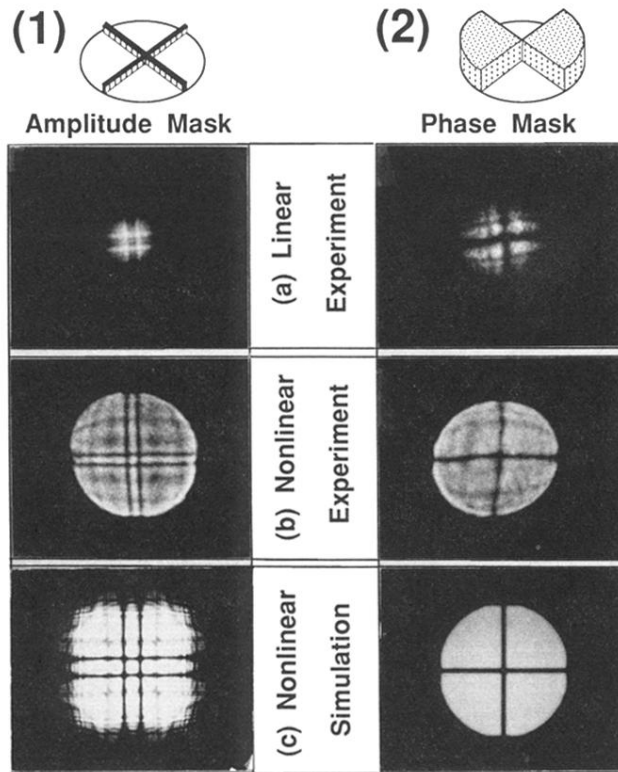


FIG. 3. Near-field cross-sectional images of the output sample face for propagation through an absorbing liquid with an amplitude cross (column 1) and a phase cross (column 2) in the incident plane.